Magnetoresistance of an Anderson Insulator of Bosons

Anirban Gangopadhyay, Victor Galitski, and Markus Müller

Phys. Rev. Lett. **111**, 026801 — Published 9 July 2013

DOI: 10.1103/PhysRevLett.111.026801

Magnetoresistance of an Anderson insulator of bosons

Anirban Gangopadhyay,[1] Victor Galitski,[1,2] and Markus Müller[3,4]

[1] *Center for Nanophysics and Advanced Materials, Department of Physics, University of Maryland, College Park, Maryland 20742-4111, USA*
[2] *Joint Quantum Institute, Department of Physics, University of Maryland, College Park, Maryland 20742-4111, USA*
[3] *The Abdus Salam International Centre for Theoretical Physics, P. O. Box 586, 34151 Trieste, Italy*
[4] *Kavli Institute for Theoretical Physics, University of California Santa Barbara, CA 93106-4030*

We study the magnetoresistance of two-dimensional bosonic Anderson insulators. We describe the change in spatial decay of localized excitations in response to a magnetic field, which is given by an interference sum over alternative tunnelling trajectories. The excitations become more localized with increasing field (in sharp contrast to generic fermionic excitations which get weakly delocalized): the localization length $\xi(B)$ is found to change as $\xi^{-1}(B) - \xi^{-1}(0) \sim B^{4/5}$. The quantum interference problem maps onto the classical statistical mechanics of directed polymers in random media (DPRM). We explain the observed scaling using a simplified droplet model which incorporates the non-trivial DPRM exponents. Our results have implications for a variety of experiments on magnetic-field-tuned superconductor-to-insulator transitions observed in disordered films, granular superconductors, and Josephson junction arrays, as well as for cold atoms in artificial gauge fields.

PACS numbers: 73.50.Jt, 74.81.Bd, 05.30.Jp, 72.20.Ee, 71.55.Jv

Transport in Anderson insulators [1, 2] is crucially determined by the properties of localized wavefunctions. Their structure is very complex, both deep in the insulator, as well as upon approaching the delocalization transition. A particularly important tool in probing the nontrivial structure of localized states in Anderson insulators is magnetoresistance. This is because a magnetic field sensitively affects the quantum interference which in turn influences quantum localization. This effect of the magnetic field has been studied extensively in the past, concentrating mostly on fermions [3, 4].

Recent experiments on disordered superconducting films provide evidence for *bosonic* insulators with localized electron pairs as carriers [5, 6]. These and other similar systems feature a giant peak in magnetoresistance (MR) [7–11]. This is often interpreted as a crossover from bosonic to fermionic transport [12, 13], even though the details remain controversial. Bosonic localization problems arise also in disordered granular superconductors in the insulating regime, in cold bosonic atoms in speckle potentials (where artificial gauge fields can mimic a magnetic field) as well as in disordered quantum magnets.

The predominant mode of transport in disordered insulators is variable-range hopping of carriers between localized excited states [14]. The spatial decay of wavefunctions describing these localized excitations determines the inelastic hopping rate and thus the resistance. At low temperature, the (phonon-assisted) hops become significantly longer than the average distance between impurity sites hosting the excitations. In this situation, one needs to know the wave-function amplitudes at distances greater than the Bohr radius of an impurity state. At these distances, the amplitude is reinforced by multiple scatterings from intermediate impurities [15] whereby many alternative paths interfere with each other [3, 4].

A perpendicular magnetic field affects the interference of the scattering paths on all length scales and modifies the localization properties. Interestingly, bosons and fermions behave very differently in this respect: while in the absence of a field fermion paths typically come with amplitudes of arbitrary signs, low energy bosonic amplitudes are positive and thus interfere in a maximally constructive way. The magnetic field suppresses this interference, yielding a strong positive magnetoresistance. It exceeds by far a largely opposite effect seen in fermions, which arises from a subtle suppression of negative interferences [16].

Despite numerous studies of fermionic MR [3, 17–19], a full understanding of the effect of magnetic field on the large-scale structure of localized wave-functions has not been obtained. In this Letter we study the bosonic cousin of this problem and show that it is amenable to a complete solution. The simplifying circumstance is the absence of additional sign-factors in the quantum interference problem, which allows a mapping to the classical statistical mechanics of directed polymers in random media (DPRM). More generally, our analysis of MR is also valid for fermionic problems, provided the interfering paths have only positive amplitudes. This arises, e.g., in the tunneling below the bottom of the conduction band in a solid semiconductor solution [20], or in fermionic impurity bands with Fermi level very close to the band bottom.

The model – Here we study a model of hard-core bosons on a square lattice,

$$H = \sum_i (\varepsilon_i - \mu) c_i^\dagger c_i - t \sum_{\langle ij \rangle} \exp\left[i \int_{\mathbf{r}_i}^{\mathbf{r}_j} d\mathbf{r} \cdot \mathbf{A} \right] c_i^\dagger c_j + \text{h.c.}, \tag{1}$$

with uniformly distributed on-site disorder in the range $\varepsilon_i \in [-W, W]$. We take $W = 1$ as the energy unit and consider weak nearest-neighbor tunneling, $t \ll W$. We fix the chemical potential to $\mu = 0$ to study a half-filled impurity band. A perpendicular magnetic field is introduced via the vector potential $\mathbf{A} = Bx\,\mathbf{e_y}$, with B being the flux per plaquette in units of the flux quantum.

We now focus on the spatial structure of an excitation localized around site i. It is characterized by the residue of the pole at $\omega \approx \epsilon_i$ of the retarded Green's function $G^R_{j,i}(\omega) = -i\int_0^\infty dt e^{i\omega t}\langle[c_j(t), c_i^\dagger(0)]\rangle$ [21]. Its decay away from the site i defines a localization length. Deep in the insulating regime, $G^R_{j,i}$ can be evaluated using a locator expansion [16]. To leading order in small hopping one obtains a sum over all paths Γ of shortest length [3], dist(ij) (cf. Fig. 1: only right-going steps are allowed)

$$S_{ji}(B) \equiv \frac{1}{t^{\mathrm{dist}(ij)}}\frac{G^R_{j,i}(\omega)}{G^R_{i,i}(\omega)}\bigg|_{\omega\to\varepsilon_i} = \sum_\Gamma e^{i\Phi_\Gamma(B)} J_\Gamma(\omega=\varepsilon_i), \quad (2)$$

which is closely analogous to the sum over paths for fermionic Anderson insulators [1]. In Eq. (2) each path Γ contributes with an amplitude

$$J_\Gamma(\omega) = \prod_{k\in\Gamma\setminus\{i\}} \frac{\mathrm{sgn}(\varepsilon_k)}{\varepsilon_k - \omega}. \quad (3)$$

and an accumulated phase $\Phi_\Gamma(B) = \int_\Gamma d\mathbf{r}\cdot\mathbf{A}$. On average, the larger the excitation energy ε_i, the faster the spatial decay of $|S_{ji}|$ [16]. Henceforth, we focus on low-frequency excitations (relevant for transport at low T) and hence set $\omega = \varepsilon_i = 0$.

Within this "forward-scattering approximation" [3], justified for $t \ll W$, bosons and fermions differ only by the presence and absence (respectively) of the factor $\mathrm{sgn}(\varepsilon_k)$ in the amplitudes (3). For bosons, the amplitudes are all positive for $\varepsilon_i = 0$. A magnetic field destroys this complete constructive interference, and thus localizes the wavefunction more [16, 18, 22]. In contrast, typical fermionic problems [3] feature amplitudes which vary in sign, depending on the number of sites on the path with $\varepsilon_i < \mu$ which are occupied in the ground state. In this case the dominant effect of a magnetic field lies in destroying negative interferences of competing paths, which tends to delocalize the wave function slightly. Both cases are readily amenable to efficient numerical studies via transfer matrices [3, 17], which we use below. The results shown in Fig. 2 illustrate the opposite trends.

The relevant quantity for transport is the *typical* spatial decay of localized excitations. Therefore one focuses on the (typical) magnetoconductance, defined as [3]

$$\Delta\sigma_N(B) = \exp\left(\overline{\ln[|{}^{Sji(B)}/_{S_{ji}(0)}|]}\right),\ N \equiv \mathrm{dist}(ij), \quad (4)$$

where the overbar denotes the disorder average. We take (i, j) on opposite corners of a square [23] (cf. Fig. 1). The linear variation with distance in Fig. 2 implies that

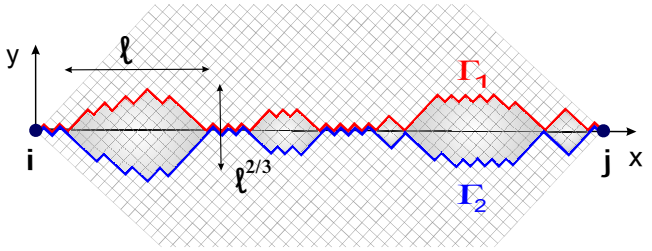

FIG. 1. The approximation of directed propagation [3] maps the wavefunction to a directed polymer. The droplet picture suggests that traces of localized wavefunctions, or low energy polymer configurations, form a string of loops of competing/interfering paths. Relevant loops of size ℓ have transverse roughness $\sim \ell^{\zeta=2/3}$). They are rare, being separated by a typical distance $\ell^{1+\theta} = \ell^{2\zeta} \gg \ell$. We show two competing paths $\Gamma_{1,2}$ and the loops/droplets they form.

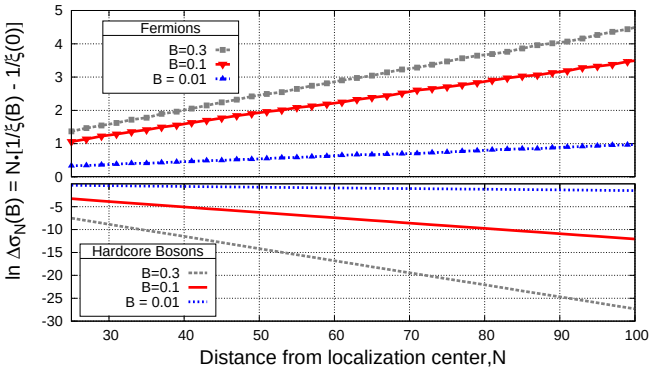

FIG. 2. Magnetoconductance of fermions and bosons as a function of distance N in a half filled impurity band ($\mu = 0$). The linear dependence implies that the magnetic flux B changes the localization length ξ. While it increases slightly for fermions, it shrinks much more substantially in bosons.

at large scales B changes the typical decay rate, i.e., the inverse localization length $1/\xi$, of the excitations.

Numerical evaluation - One numerically evaluates $S_{ji}(B) \equiv S_{x_j,y_j}(B)$ (with i as origin) by recursion

$$S_{x+1,y}(B) = V_{x+1,y}\left[e^{i\phi_-}S_{x,y-1}(B) + e^{i\phi_+}S_{x,y+1}(B)\right] \quad (5)$$

with $\phi_\pm = \int_{\Gamma_\pm}\mathbf{A}\cdot d\mathbf{r}$, where $\Gamma_\pm : (x, y\pm1) \to (x+1, y)$ are straight paths along the lattice links and $V_{x,y} = {}^1/_{|\varepsilon_{x,y}|}$. $\Delta\sigma_N(B)$ evaluated from this varies as B^2N^3 for small (B, N) and shows a sharp crossover to $NB^{4/5}$ at larger fields/distances (cf. Fig. 3). The data for different N is found to collapse onto a scaling function

$$|\ln\Delta\sigma_N(B)| = N^{-1/3}\Phi\left(NB^{3/5}\right), \quad (6)$$
$$\Phi(x \ll 1) = b_1 x^{10/3}\ ;\ \ \Phi(x \gg 1) = b_2 x^{4/3},$$

with $b_1 \approx 0.31, b_2 \approx 0.56$. This scaling is expected theoretically from the physics of directed polymers (DPRM), as we explain below.

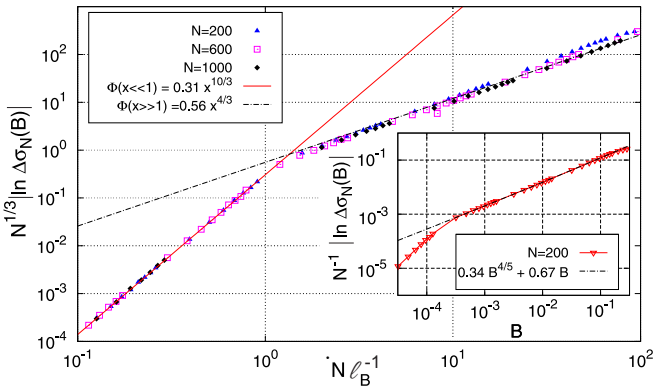

FIG. 3. Scaling of the magnetoconductance, $\Delta\sigma$, with distance N and flux per plaquette, B. The crossover from the perturbative regime $|\ln \Delta\sigma_N(B)| \sim B^2N^3$ to the non-perturbative regime $|\ln \Delta\sigma_N(B)| \sim NB^{4/5}$ occurs at $N \sim \ell_B$, where many successive interfering loops start contributing. Inset: change of inverse localization length for $N = 200$, and best fit to the leading two terms in Eq. (11), $\xi^{-1}(B)-\xi^{-1}(0) = c_1B^{4/5} + c_2B$.

Mapping to directed polymers - By virtue of the positive path amplitudes $S_{ji}(B = 0)$ can be interpreted as the partition sum of a DPRM in 1+1 dimensions [24, 25] with random onsite energies $\ln|\varepsilon_i|$ (at temperature $T = 1$) and ends fixed at sites i and j. Each polymer configuration corresponds to a directed path Γ of the expansion (2).

In low dimensions, DPRM exhibit a pinned phase at large scales, as the random potential is relevant under renormalization [26, 27]. Beyond a characteristic pinning scale L_c (of the order of the lattice scale here), the random potential competes strongly with the polymer's entropic elasticity and induces roughness exceeding that of random walks: On longitudinal scales ℓ, typical transverse excursions of configurations grow as ℓ^ζ with $\zeta > 1/2$. A low energy excitation that differs from dominant configurations on scale ℓ, has typical excitation energy $E(\ell) \sim \ell^\theta$, with energy exponent $\theta = 2\zeta - 1$ [28]. In 1+1 dimensions (MR in 2d), the value $\zeta = 2/3$ is known exactly [29], while $\zeta_{3d} \approx 0.62$ is known numerically [30].

When $B \neq 0$, the polymer configurations acquire complex weights. Studies of ζ and θ exponents of complex DPRM [31] suggest that the scalings of the pinned phase do not change with complex weights. In fact, for fermions at $B = 0$, where negative weights are abundant, there is numerical evidence that the wavefunctions are still governed by DPRM exponents [32–34]. We thus assume that the DPRM exponents hold for finite fields as well.

It is interesting to note that for weak fields, Eq. (5) admits a continuum limit, where S obeys the equation

$$D_xS = D_y^2S + V(x, y)S, \tag{7}$$

with a δ-correlated random potential term $V(x, y)$ and $D_{\alpha=(x,y)} \equiv \partial_\alpha - iA_\alpha(x, y)$ being the gauge-covariant derivative (in Landau gauge $A_y = 0$). This generalizes the Kardar-Parisi-Zhang (KPZ) equation [35] to the presence of complex potentials $V \to V + iA_x$, and may render bosonic MR amenable to a field theoretic analysis similar to Refs. [36, 37]. However, a rigorous study of this modified KPZ equation is not attempted here.

In DPRM language, the magnetoconductance can be cast as a thermodynamic average of the phase factors $e^{i\Phi_\Gamma(B)}$ over polymer configurations, and the ratio of amplitudes S_{ji} takes the manifestly gauge-invariant form:

$$\left|\frac{S_{ji}(B)}{S_{ji}(0)}\right|^2 = \left[\frac{\sum_{\Gamma,\Gamma'} e^{-E_\Gamma-E_{\Gamma'}}\cos\left(BA_{\Gamma\Gamma'}\right)}{\sum_{\Gamma,\Gamma'} e^{-E_\Gamma-E_{\Gamma'}}}\right]. \tag{8}$$

Here $E_\Gamma = \sum_{k\in\Gamma\setminus i}\ln|\varepsilon_k|$ is the energy of configuration Γ, and $A_{\Gamma\Gamma'}$ is the oriented area enclosed by Γ and Γ'.

MR in weak fields - For weak fields or short distances one can evaluate $\Delta\sigma_N(B)$ perturbatively in B. Typical loops of linear extent ℓ enclose a flux $\sim B\ell^{1+\zeta}$. Of the N/ℓ possible independent loops only a fraction $\sim \ell^{-\theta}$ interfere significantly, cf. Fig 1, and are thus sensibly affected by B. As long as $N \ll \ell_B \equiv B^{-\frac{1}{\zeta+1}}$ the dominant contribution to Eqn. 8 comes from the largest loops of length $\ell \sim N$, which nevertheless enclose only a fraction of a flux quantum. This results in the magnetoconductance (4) $\Delta\sigma_N \propto -N^{-\theta}(BN^{1+\zeta})^2 = -B^2N^3$. The roughness exponent drops out of this perturbative result. We therefore recover the scaling previously predicted for interfering paths with positive weights [3], even though those assumed random walk scaling, $\zeta = 1/2$.

MR in strong fields - For $N > \ell_B$, DPRM scalings show more clearly in the magnetoresponse. The dominant contribution to $\Delta\sigma_N$ comes from reduced interference in loops of length ℓ_B, each of which decreases $\Delta\sigma_N$ by $O(1)$. Larger loops contribute similarly, but their probability to interfere significantly decreases as $\ell^{-\theta}$. On the other hand, smaller loops, albeit more abundant and likely to interfere, enclose a small fraction of a flux quantum, and thus have a negligible effect. The contribution from loops of size ℓ_B gives rise to an extensive $\ln(\Delta\sigma_N)$ proportional to the density of significantly interfering loops,

$$\frac{\ln\Delta\sigma_N}{N} \equiv -\Delta\left[\frac{1}{\xi}\right] \sim -\ell_B^{-1}\ell_B^{-\theta} = -B^{\frac{1+\theta}{1+\zeta}} = -B^{\frac{2\zeta}{1+\zeta}}. \tag{9}$$

This is equivalent to a reduction of the inverse localization length by $B^{4/5}$ in 2d. In $3d$ the same arguments yield an exponent $2\zeta/(1 + \zeta) \approx 0.765$. Both exceed the value 2/3 obtained upon neglecting pinning and assuming random walk scaling with $\zeta = 1/2$. The latter is valid only for a limited number of weak scatterings [3, 20].

So far we have discussed the leading scaling with magnetic field. However, the numerical data show small subleading corrections, cf. inset of Fig. 3. Those arise from spatially overlapping loops. To understand their effect, we introduce a hierarchical model built on the droplet theory for directed polymers [27, 28]. At a given length

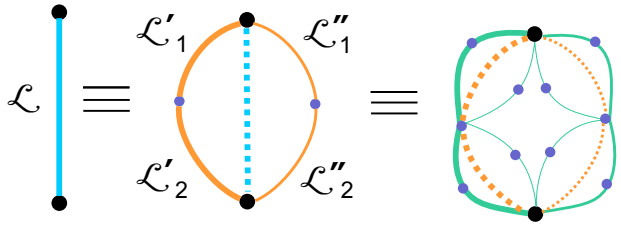

FIG. 4. Hierarchical droplet model: At each level of the hierarchy, a parent loop $\mathcal{L}$ (composed of a dominant and subdominant branch) is split into four subloops, two forming the dominant branch ($\mathcal{L}'_{1,2}$, thicker line), and two forming the subdominant branch ($\mathcal{L}''_{1,2}$, thinner lines), cf. Eq. (10). The parent levels are indicated by dashed lines. The dots indicate the splitting into two successive loops at the next level.

scale L, the polymer has a preferred set of configurations, which usually competes with alternative, subdominant sets of paths. The leading family of subdominant paths has $O(L^\theta)$ higher free energy and wanders off the dominant configuration by L^ζ, enclosing a typical loop area $O(L^{1+\zeta})$. This pattern repeats at all length scales. We simplify this phenomenology by considering a model where loops and alternative paths are restricted to lengths $L_k = N2^{-k}$ where $N \gg 1$ is the fixed distance between endpoints. Each parent loop $\mathcal{L}$ of size L_k is composed of a dominant and a subdominant set of paths, each consisting of two successive loops $\mathcal{L}'_{1,2}$ and $\mathcal{L}''_{1,2}$ of size L_{k+1}, cf. Fig. 4. We define the propagation amplitude and build in DP scaling by defining

$$S^k_{\mathcal{L}} = S^{k+1}_{\mathcal{L}'_1} S^{k+1}_{\mathcal{L}'_2} + e^{-f_{\mathcal{L}} L_k^\theta} e^{i a_{\mathcal{L}} B L_k^{1+\zeta}} S^{k+1}_{\mathcal{L}''_1} S^{k+1}_{\mathcal{L}''_2}, \quad (10)$$

and setting all $S^k_{\mathcal{L}} = 1$ for k with $L_k \lesssim \ell_B$ [38]. $f_{\mathcal{L}} > 0$ and $a_{\mathcal{L}}$ are random variables of order $O(1)$, with a probability density $\rho(f_{\mathcal{L}}, a_{\mathcal{L}})$, assumed to be i.i.d. for all loops $\mathcal{L}$. The magnetoresistance is then defined as $\Delta\sigma_N = \overline{\ln(|S_{0N}(B)/S_{0N}(0)|)}$. Note that significant interference between the paths $\mathcal{L}'$ and $\mathcal{L}''$ in Eq. 10 occurs only in rare 'active loops' $\mathcal{L}$ for which $f_{\mathcal{L}} L^\theta \lesssim 1$.

In contrast to the hierarchical lattices analyzed in Ref. 39, we *explicitly* include here the known scaling of excitation energies and areas of loops, which are essential to discuss magnetoresponse.

The perturbative scaling $\Delta\sigma_N \sim B^2 N^3$ is easy to obtain in this model. In the non-perturbative regime ($N \gg \ell_B \gg 1$), using that active loops are sparse, one can expand $\ln \Delta\sigma_N(B)$ in powers of the density of active loops of linear size ℓ_B, [40]

$$\frac{\ln \Delta\sigma_N(B)}{N} = -B^{\frac{2\zeta}{1+\zeta}} [c_1 + c_2 B^{\frac{\theta}{1+\zeta}} + c_3 B^{\frac{2\theta}{1+\zeta}} + \cdots], \quad (11)$$

where the constants c_i depend only on the distribution $\rho(f, a)$. As in the cluster expansion for interacting particles, one obtains a term of $O\left(B^{(1+n\theta)/(1+\zeta)}\right)$ from contributions with n active loops. The leading coefficient c_1 is positive definite, and we found $c_2 > 0$, independently of our choice of the distribution $\rho(f, a)$. Subleading terms due to interfering loops thus enhance the negative MR of bosons. This may explain a similar effect seen in the numerical data on the original lattice (inset of Fig. 3), where a fit yields $c_1 \approx 0.34, c_2 \approx 0.67$. In practice, $\ln \Delta\sigma$ thus appears to follow a power law with slightly larger exponent than 4/5.

Experimental consequences - At low T the boson transport proceeds by variable-range hopping, whose resistance, at fixed T, depends on the localization length as $R(\xi) = \rho \exp(A/\xi^\alpha)$, with $\alpha = 1/2$ (with Coulomb gap) and $2/3$ (constant density of states in $d = 2$) [14]. According to (9) a perpendicular magnetic field reduces the localization length ξ according to

$$1/\xi(B) \approx 1/\xi_0 + \Delta[1/\xi](B), \quad B_{\min} \lesssim B \equiv \frac{\hat{B} a^2}{\phi_0}, \quad (12)$$

where we recall the definition of B in terms of the physical field $\hat{B}$, the spacing a between impurities, and the relevant flux quantum ϕ_0. Here $B_{\min} = (R_{\rm hop}/a)^{-5/3} = [\ln(R(0)/\rho)\xi_0/a]^{-5/3}$ is required to access the strong MR regime, in which $\ell_B = aB^{-3/5}$ is shorter than the typical hopping distance, $R_{\rm hop}$. At smaller fields the perturbative results above predict a relative increase of resistance proportional to $B^2(R_{\rm hop}/a)^3$, which is dominated by the response of a few rare elementary resistors. In contrast, in the strong MR regime, to lowest order in B the resistance increases by the large factor

$$R(B)/R(0) = [R(0)/\rho]^{\alpha\, \xi_0 \Delta[1/\xi]}, \quad B_{\min} \lesssim B. \quad (13)$$

For $B \ll 1$, the exponent is $\alpha c_1 \xi_0 B^{4/5}$. For $B \to 1$, subleading terms further add to this, yielding values as big as $0.3\alpha\xi_0$, cf. Fig. 3. These effects are even much stronger in presence of a Coulomb gap [41]. As resistances up to $R(0)/\rho \sim 10^6$ are easily measurable, and localization lengths $\xi \lesssim 2$ are safely within the regime of applicability of forward scattering our theory can reliably predict *strongly positive* MR of bosons, with enhancement factors of up to two or three orders of magnitude.

In contrast, the analogous fermionic problem exhibits *negative* MR, with much smaller maximal amplitudes, cf. Fig. 2. The importance of the bosonic effect suggests that it is a key ingredient in the MR peak observed in superconducting films with preformed pairs [7]. Those experiments are usually conducted close to criticality where $\xi \gg a$. In that case our theory still applies qualitatively in weak fields where $\hat{B}\xi^2$ (upon coarsegraining to scales $\sim \xi$). However, the MR receives additional positive contributions at larger fields $\hat{B} \gtrsim \phi_0/\xi^2$, which affect the bosonic ground state *within* the correlation volume.

Apart from experiments of MR in condensed matter, it would be very interesting to probe magnetoresponse and its sensitivity on quantum statistics using cold atoms, e.g. employing synthetic gauge fields.

After this work was completed, we became aware of Ref. [42], which also discusses similar magnetoresistance phenomena for single particle variable-range hopping.

We would like to thank A. Dobrinevski, P. Le Doussal and B.I. Shklovskii for very useful discussions. This research was supported by NSF DMR-0847224 (A.G.) and DOE-BES DESC0001911 (V. G.) and NSF-KITP-12-183 (M.M.).

[1] P. W. Anderson, Phys. Rev. **109**, 1492 (1958).
[2] E. Abrahams, ed., *50 years of Anderson Localization* (World Scientific, 2010).
[3] V. Nguen, B. Spivak, and B. Shklovskii, Sov. Phys. JETP **62**, 1021 (1985); B. Shklovskii and B. Spivak, *Hopping Transport in Solids*, edited by M. Pollak and B. Shklovskii (Elsevier Science, 1991).
[4] M. Kardar, *Statistical Physics of Fields* (Cambridge University Press, 2007).
[5] B. Sacépé, T. Dubouchet, C. Chapelier, M. Sanquer, M. Ovadia, D. Shahar, M. Feigel'man, and L. Ioffe, Nature Phys. **7**, 239 (2011).
[6] V. F. Gantmakher, Low Temp. Phys. **37(1)**, 59 (2011).
[7] G. Sambandamurthy, L. Engel, A. Johansson, and D. Shahar, Phys. Rev. Lett. **92**, 107005 (2004).
[8] M. A. Paalanen, A. F. Hebard, and R. R. Ruel, Phys. Rev. Lett. **69**, 1604 (1992).
[9] T. I. Baturina, A. Y. Mironov, V. M. Vinokur, M. R. Baklanov, and C. Strunk, Pis' ma v ZhETF **88**, 867 (2008).
[10] Y.-H. Lin and A. M. Goldman, Phys. Rev. Lett. **106**, 127003 (2011).
[11] M. A. Steiner, G. Boebinger, and A. Kapitulnik, Phys. Rev. Lett. **94**, 107008 (2005).
[12] J. Mitchell, A. Gangopadhyay, V. Galitski, and M. Müller, Phys. Rev. B **85**, 195141 (2011).
[13] T. Chen, B. Skinner, and B. I. Shklovskii, Phys. Rev. B **86**, 045135 (2012).
[14] A. L. Efros and B. I. Shklovskii, *Electronic properties of doped semiconductors* (Springer Berlin, 1984).
[15] B. I. Shklovskii, JETP Lett **36**, 287 (1982).
[16] M. Müller, arXiv: 1109.0245v1 (2011).
[17] E. Medina and M. Kardar, Phys. Rev. B **46**, 9984 (1992).
[18] H. L. Zhao, B. Z. Spivak, M. P. Gelfand, and S. Feng, Phys. Rev. B **44**, 10760 (1991).
[19] O. Entin-Wohlman, U. Sivan, and Y. Imry, Phys. Rev. Lett **60**, 1566 (1988).
[20] B. Shklovskii and A. L. Efros, Sov. Phys. JETP **57**, 470 (1983).
[21] This follows immediately from the Lehmann representation of the Green's function.
[22] S. Syzranov, A. Moor, and K. Efetov, Phys. Rev. Lett. **108**, 256601 (2012).
[23] This comes closest to disordered, statistically isotropic lattices. [3] Note that the Hamming distance N is the Euclidean distance measured in units of one half of the plaquette diagonal.
[24] D. A. Huse and C. Henley, Phys. Rev. Lett. **54**, 2708 (1985).
[25] T. Halpin-Healy and Y.-C. Zhang, Phys. Rep. **254**, 215 (1995).
[26] A. I. Larkin and Y. N. Ovchinnikov, J. Low Temp. Phys. **34**, 409 (1979).
[27] D. S. Fisher and D. A. Huse, Phys. Rev. B **43**, 10728 (1991).
[28] T. Hwa and D. Fisher, Phys. Rev. B **49**, 3136 (1994).
[29] D. A. Huse, C. Henley, and D. Fisher, Phys. Rev. Lett. **55**, 2924 (1985).
[30] L.-H. Tang, B. M. Forrest, and D. E. Wolf, Phys. Rev. A **45**, 7162 (1992).
[31] E. Medina, M. Kardar, Y. Shapir, and X. Wang, Phys. Rev. Lett. **62**, 941 (1989).
[32] J. Prior, A. M. Somoza, and M. Ortuno, Phys. Rev. B **72**, 024206 (2005).
[33] J. Prior, A. M. Somoza, and M. Ortuno, Eur. Phys. J B **70**, 513 (2009).
[34] C. Monthus and T. Garel, J. Phys. A : Math. Theor. **45**, 095002 (2012).
[35] M. Kardar, G. Parisi, and Y.-C. Zhang, Phys. Rev. Lett. **56**, 889 (1986).
[36] D. Forster, D. R. Nelson, and M. J. Stephen, Phys. Rev. A **16**, 732 (1977).
[37] E. Frey and U. C. Täuber, Phys. Rev. E **50**, 1024 (1994).
[38] See Supplement, Sec. IA, for a discussion of the short scale cut-off, and an alternative definition of the hierarchical model with no restriction on loop lengths.
[39] B. Derrida and R. B. Griffiths, Europhys. Lett. **8**, 111 (1989).
[40] See Supplement, Secs. IB and II for details.
[41] Upon excluding resonances by constraining $\epsilon_i \in [-1,-1/2]\cup[1/2,1]$, positive MR is enhanced, and the exponent in Eq. (13 reaches values up to $\sim 0.6\alpha\xi_0$.
[42] L. B. Ioffe and B. Z. Spivak, arXiv: 1305.1895 (2013).